Integrated Multiquadric Radial Basis Function Approximation Methods

S. A. Sarra

Department of Mathematics, Marshall University
One John Marshall Drive
Huntington, WV 25755, U.S.A.

Abstract——Promising numerical results using once and twice integrated radial basis functions have been recently presented. In this work we investigate the integrated radial basis function (IRBF) concept in greater detail, connect to the existing RBF theory, and make conjectures about the properties of IRBF approximation methods. The IRBF methods are used to solve PDEs. © 2006 Elsevier Science Ltd. All rights reserved.

Keywords——Radial basis function, Interpolation, Numerical partial differential equations.

1. INTRODUCTION

Over the last several decades radial basis functions (RBFs) have been found to be widely successful for the interpolation of scattered data. More recently, the RBF methods have emerged as an important type of method for the numerical solution of partial differential equations (PDEs) [1,2]. RBF methods can be as accurate as spectral methods without being tied to a structured computational grid. This leads to ease of application in complex geometries in any number of space dimensions.

A *radial basis function* $\phi(r)$ is a continuous univariate function that has been radialized by composition with the Euclidean norm on $\mathbb{R}^d$. RBFs may or may not contain a free parameter called the *shape parameter* which we denote by c. Well-known RBFs without a shape parameter are the *polyharmonic splines*

$$\phi(r) = \begin{cases} r^k, & k \notin 2\mathbb{N}, \\ r^{2k} \log r, & k \in \mathbb{N}. \end{cases} \tag{1}$$

The polyharmonic splines are alternatively known as surface splines or in the case of $\phi(r) = r^{2k} \log r$, thin-plate splines. This class of RBF typically approximates with algebraic convergence rates. In this work we are interested in RBFs that contain a shape parameter, but we will make some connections between the two types. Some commonly used RBFs containing a shape parameter are listed in Table 1. This class can exhibit spectral rates of convergence. The previously mentioned RBFs have global support. However, this is not a necessity as compactly

Table 1. Global, infinitely smooth RBFs.

Name of RBF	Definition
Multiquadric (MQ)	$\phi(r,c) = \sqrt{1 + c^2 r^2}$
Inverse Quadratic (IQ)	$\phi(r,c) = \dfrac{1}{(1 + c^2 r^2)}$
Gaussian (GA)	$\phi(r,c) = e^{-c^2 r^2}$

supported RBFs, such as the Wendland functions [3], are also well known. The interested reader is referred to the recent book by Buhmann [4] for more basic details about RBFs.

RBF methods for PDEs are based on a scattered data interpolation problem. Let Ξ be a finite distinct set of points in $\mathbb{R}^d$, which are traditionally called *centers* in the language of RBFs. The idea is to use linear combinations of translates of one function $\phi(r)$ of one real variable which is centered at $\xi \in \Xi$ to approximate a function f as

$$s(x) = \sum_{i=0}^{N} \lambda_i \phi\left(\|x - \xi_i\|_2\right), \qquad x \in \mathbb{R}^d. \tag{2}$$

The most attractive feature of the RBF methods is that the location of the centers can be chosen arbitrarily in the domain of interest. The interpolation problem is to find expansion coefficients, λ_i, so that

$$s|_\Xi = f|_\Xi \tag{3}$$

for given data $f|_\Xi$. That is, they are obtained by solving the linear system

$$H\lambda = f, \tag{4}$$

where the elements of the *interpolation matrix* H are $h_{i,j} = \phi(\|\xi_i - \xi_j\|_2)$ for $i, j = 0, 1, \ldots, N$.

For the RBFs in Table 1 the interpolation matrix H can be shown to be invertible [5]. However, the interpolation matrix is often very ill-conditioned and it may be difficult to deal with the system numerically. The conditioning of H is measured by the *condition number* defined as

$$\kappa(H) = \|H\| \left\|H^{-1}\right\| = \frac{\sigma_{\max}}{\sigma_{\min}}, \tag{5}$$

where σ are the singular values of H. The reason that H is in practice usually ill-conditioned is due to what Schaback [6] has assigned the name of the *uncertainty principle*. The uncertainty principle states that with RBF approximation methods we cannot simultaneously have good conditioning and good accuracy.

In general, small shape parameters produce the most accurate results, but are also associated with a poorly conditioned interpolation matrix. For fixed values of the shape parameter, the conditioning of the interpolation matrix deteriorates as the separation distance between centers, defined as

$$q_\Xi = \frac{1}{2} \min_{i \neq j} \|\xi_i - \xi_j\|_2, \tag{6}$$

decreases. Obviously, by increasing the number of centers used, we decrease q_Ξ. Many researchers [7–9] have searched for an algorithm to specify an "optimal" shape parameter, i.e., a value that produces maximal accuracy while maintaining numerical stability. However, determining the optimal shape parameter is still an open question and it is often chosen by brute force in applications. The shape parameter is modified until the resulting interpolation matrix has a condition number below a threshold. Using 32-bit double precision floating point arithmetic, standard linear algebra packages typically began to fail when $\kappa(H) = \mathcal{O}(10e17)$, which we refer to as the floating point limit.

Recently, some promising numerical results [10–12] using once and twice integrated radial basis functions have been presented. In these works, the authors argued heuristically that the smoothing process of integration led to more accurate methods than those using the standard nonintegrated RBFs. Since the convergence rates of the MQ RBFs drop with increasing order of differentiation [13,14], integration of the basis functions counters this trend. Subsequently, other researchers have used the idea. In [15] twice integrated MQ RBFs were used to solve one-dimensional boundary value problems. In [16] a volumetric integral RBF method is formulated for time-dependent PDEs. Unfortunately, in [15] the methods were only discussed for a fixed constant value of the shape parameter. We are interested in the properties of the IRBF methods over the entire range of the shape parameter. In [10–12] a larger range of the shape parameter was considered but the limiting cases $c \to 0$ and $c \to \infty$ were not discussed. In this work we take a closer look at integrated RBFs and examine their properties over the full range of the shape parameter including the limiting cases. Additionally, we discuss the invertibility of the interpolation matrix for the integrated RBFs.

The focus of this work is on the integrated family of RBFs based on the MQ RBF which we refer to as the parent of the integrated family. The MQ was chosen because it is very popular in applications and many theoretical results exist for the MQ [8]. We note that integrated RBF families based on other parent RBFs such as the IQ and GA have many similar properties as the MQ family, but in several aspects there are marked differences.

2. INTEGRATED RBFS

Let the notation $\phi^n(r, c)$ represent a global infinitely differentiable RBF containing a shape parameter c that has been integrated ($n > 0$) or differentiated ($n < 0$) n times with respect to r. We refer to these RBFs as integrated RBFs (IRBFs), as it is the case $n > 0$ that we are interested in for use in approximations. IRBFs are easily found using a computer algebra system. For reference, we list the first four members of the integrated RBF family based on the MQ RBF

$$\phi^1 = \frac{cr\sqrt{1 + c^2 r^2} + \sinh^{-1}(cr)}{2c}, \tag{7}$$

$$\phi^2 = \frac{\left(-2 + c^2 r^2\right)\sqrt{1 + c^2 r^2} + 3cr\sinh^{-1}(cr)}{6c^2}, \tag{8}$$

$$\phi^3 = \frac{cr\sqrt{1 + c^2 r^2}\left(-13 + 2c^2 r^2\right) + 3\left(-1 + 4c^2 r^2\right)\sinh^{-1}(cr)}{48c^3}, \tag{9}$$

$$\phi^4 = \frac{\sqrt{1 + c^2 r^2}\left(16 - 83c^2 r^2 + 6c^4 r^4\right) + 15cr\left(-3 + 4c^2 r^2\right)\sinh^{-1}(cr)}{720c^4}. \tag{10}$$

For small c, members of the MQ IRBF family have the series expansion

$$\phi^n(r) = \sum_{m=M}^{\infty} a_m r^{n+2m} c^{2m}, \tag{11}$$

where $M = -\lfloor n/2 \rfloor$. For example, ϕ^4 of the IMQ (integrated multiquadric) family has the expansion

$$\phi^4 = \frac{1}{45c^4} - \frac{r^2}{6c^2} + \frac{r^4}{24} + \frac{r^6 c^2}{720} + \cdots \tag{12}$$

and ϕ^5 has

$$\phi^5 = \frac{r}{45c^4} - \frac{r^3}{18c^2} + \frac{r^5}{120} + \frac{c^2 r^7}{5040} + \cdots . \tag{13}$$

(a) Graph of evenly integrated IMQ $\phi^4(r)$ for various values of the shape parameter.

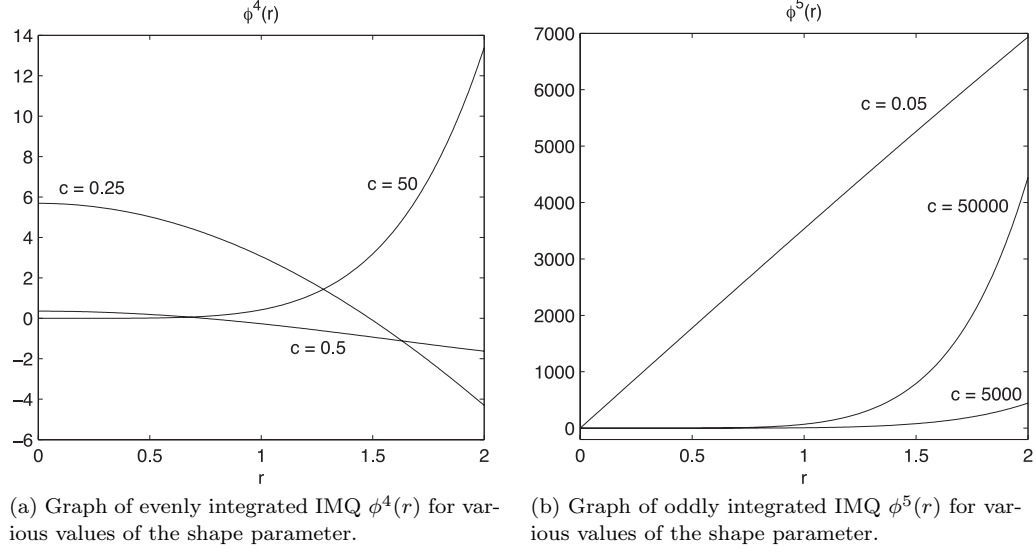(b) Graph of oddly integrated IMQ $\phi^5(r)$ for various values of the shape parameter.

Figure 1.

As c approaches zero the even (n even) IMQs approach a large constant and are infinite for $c = 0$. The odd IMQs approach a large multiple of $\phi(r) = r$. For large c the odd IMQs are approximately

$$\phi^n(r) \approx cr^{n+1} + \frac{1}{c}r^{n-1}\log r, \qquad n \text{ odd}, \tag{14}$$

and the even IMQs are approximately

$$\phi^n(r) \approx cr^{n+1}, \qquad n \text{ even}. \tag{15}$$

That is, for large c, the odd IMQs are approximately a polyharmonic spline perturbed by a multiple of an even power of r and the even IMQs are a large multiple of a polyharmonic spline. Figure 1 illustrates the shape of ϕ^4 and ϕ^5 for various values of the shape parameter.

Derivatives of mth order with respect to x_k, $k = 1, \ldots, d$, of interpolant (2) may be calculated in a straightforward manner at centers $\xi_j \in \Xi$ as

$$\frac{\partial^m}{\partial x_k^m}s(\xi_j) = \sum_{i=0}^{N}\lambda_i\frac{\partial^m}{\partial x_k^m}\phi^n\left(\|\xi_j - \xi_i\|_2\right). \tag{16}$$

Elementary calculus allows us to find derivatives of any order, and in any number of space dimensions, in terms of the other members of the IRBF family. For example, the first derivative with respect to x_k may be calculated as

$$\frac{\partial\phi^n}{\partial x_k} = \phi^{(n-1)}(r, c)\frac{\partial r}{\partial x_k},$$

where $r = \|\mathbf{x}\|_2$. Likewise, the second derivative with respect to x_k is

$$\frac{\partial^2\phi^n}{\partial x_k^2} = \phi^{(n-1)}(r, c)\frac{\partial^2 r}{\partial x_k^2} + \phi^{(n-2)}(r, c)\left(\frac{\partial r}{\partial x_k}\right)^2.$$

Next we discuss the stability and the approximation properties of the IRBF methods based on the MQ RBF. Most of the properties of the IRBF methods depend on whether the basis functions have been integrated an even or an odd number of times. In the numerical examples which follow, we measure the error over a range of shape parameters in a domain Ω in the maximum norm as

$$E(c) = \max_{\Omega}|s(x) - f(x)|.$$
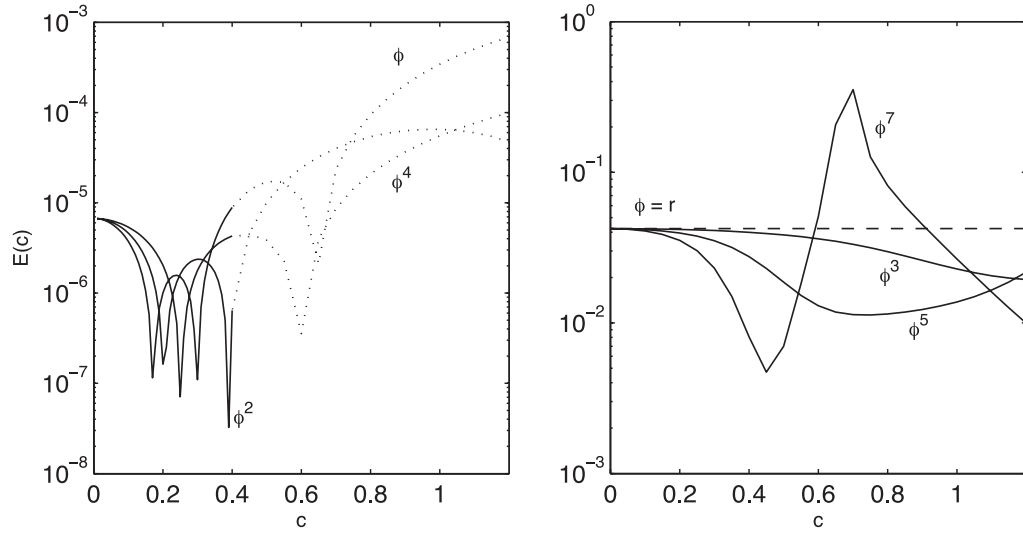
3. BEHAVIOR AS A FUNCTION
OF THE SHAPE PARAMETER

3.1. Approximation

The limiting case as $c \to 0$ has previously been examined in [17] for RBFs containing a shape parameter that has a series expansion of form (11) with $n = 0$. Among many other RBFs, the analysis of [17] includes the MQ, IQ, and GA. In the limit $c \to 0$ the RBFs become a constant, a situation that is referred to as the flat limit. In [17] it was shown that for a distinct set of centers in one dimension, the RBF interpolant exists as $c \to 0$ and is equal to the Lagrange interpolating polynomial on that set of nodes given the invertibility of two associated matrices. Although not proven, it was conjectured that the associated matrices are nonsingular for all standard choices of $\phi(r)$, including the IQ, MQ, and GA. In two dimensions, it was found that the limiting interpolant may not exist, especially on tensor-product grids. However, when the limit does exist, it depends on $\phi(r)$ and is a multivariate finite-order polynomial. The analysis of the two-dimensional case was continued in [18] and extended by Schaback in [19]. The limiting case as $c \to \infty$ has not received much attention in the literature except for the acknowledgment that RBFs with "large" shape parameters produce poor approximations which are comparable to low-order local methods.

To numerically explore the IRBF methods with shape parameters for which the interpolation matrix is too poorly conditioned to use standard methods, we use the Contour-Padé (CP) algorithm [20]. The CP algorithm stably calculates the RBF approximation, for a small number of centers, for all values of c including at the limiting value $c = 0$. Details of the algorithm may be found in [20].

We now consider the quality of approximations produced by the IRBF for both small and large c. The cases of n even and n odd are different and are discussed separately.

In one dimension, the result of Theorem 3.1 in [17] holds if we replace the hypothesis that the basis functions have the small c expansion (11) with $n = 0$ with the same hypothesis with $n \geq 0$ and n is even. Thus if some auxiliary conditions are satisfied as specified in [17], the evenly integrated IMQ approximants are equivalent to the Lagrange approximant in the limit $c \to 0$.

(a) n even with the direct method (dotted) and Contour-Padé algorithm (solid).

(b) n odd compared with linear splines $\phi(r) = r$.

Figure 2. Small shape parameter in 1d. Max error vs. shape parameter from interpolating $f(x) = \cos(\pi x)$ with $N = 10$ uniformly spaced centers to $x_0 = 0.25$ using IMQs ϕ^n. Note the different scales.

(a) ϕ^n for n even. Direct dotted, Contour-Padé solid.
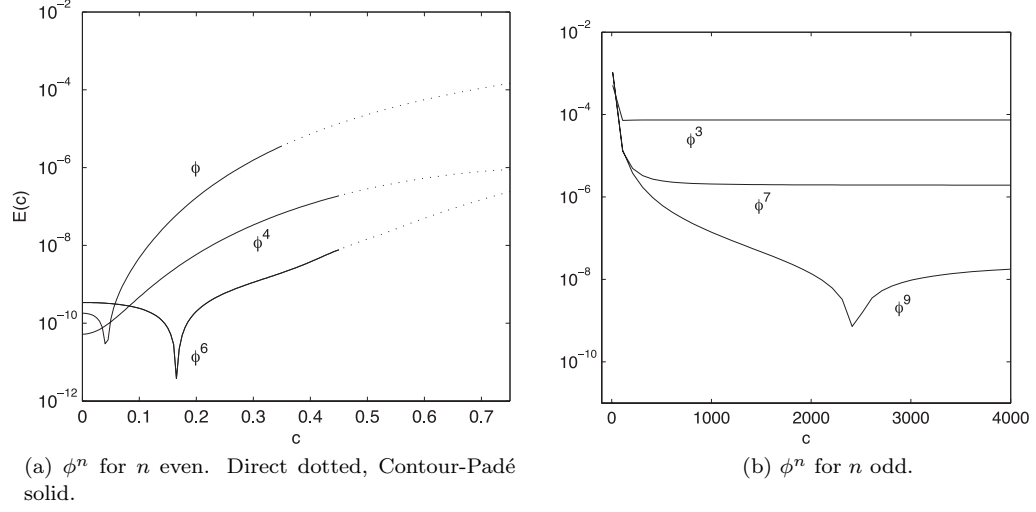
(b) ϕ^n for n odd.

Figure 3. Scattered 2d derivative approximation. Errors at the point $(0, 0.2)$ (shaded point in Figure 4) from calculating $\frac{\partial f}{\partial x}$ for $f(x, y) = \exp(x/2 + y/4)$ on the unit circle with 54 centers distributed as in Figure 4.
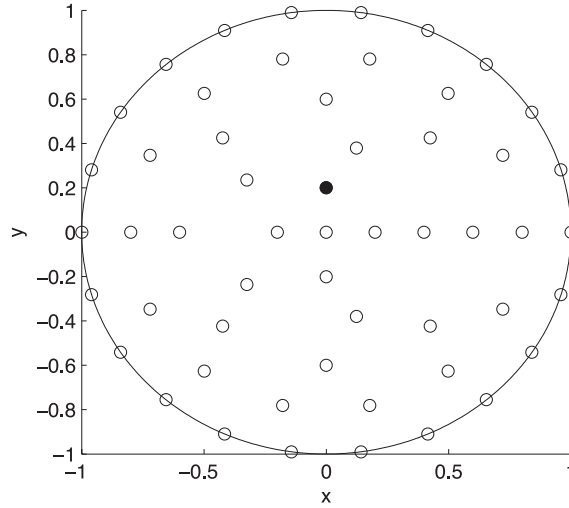

Figure 4. 54 scattered nodes one the unit circle.

Thus, for even IMQ interpolation methods which include the parent RBF, we get something familiar as c approaches zero. As $c \to 0$ the condition number of the interpolation matrix for the even IMQs becomes unbounded which prevents the evaluation of the interpolant by standard methods. For small N the Contour-Padé algorithm is applicable and we use it in such an example with results shown in Figure 2a to illustrate the equivalence of all the even IMQ interpolants as $c \to 0$. For $d > 1$, we no longer have equivalence with the Lagrange approximant as $c \to 0$. This is illustrated in Figure 3 with the aide of the CP algorithm for the approximation of a partial derivative at scattered centers on the unit circle. When the approximant exists, it depends on the particular even IMQ family member that is used.

For large c, the even IMQ approximants behave as expected as their large c approximations, the polyharmonic splines (15). This large c behavior is illustrated by an example in Figure 5a.

As $c \to 0$ the odd members of the IMQ family approach a multiple of the linear polyharmonic spline $\phi(r) = r$. For small $c > 0$ the odd IMQ methods approximate with the accuracy of the linear splines. An example illustrating the small shape accuracy of the odd IMQs is in Figure 2b.
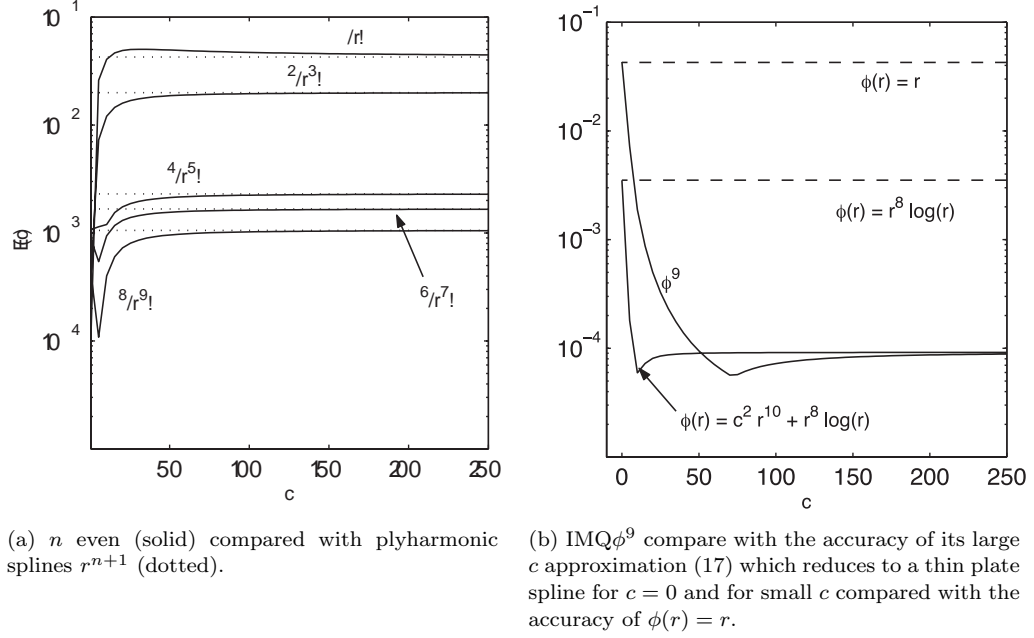
(a) n even (solid) compared with plyharmonic splines r^{n+1} (dotted).

(b) IMQϕ^9 compare with the accuracy of its large c approximation (17) which reduces to a thin plate spline for $c = 0$ and for small c compared with the accuracy of $\phi(r) = r$.

Figure 5. Interpolation maximum error vs. shape parameter for "large" shape parameters with IMQs ϕ^n. The function $f(x) = \exp(x^3) + \cos(2x)$ at $N = 20$ equally spaced interpolation points on $[-1, 1]$ was interpolated to a finer evenly spaced grid with $N = 100$.

For large c, the odd IMQ methods approximate as if the basis functions are as in equation (14). If equation (14) is multiplied by c we get

$$\phi^n \approx c^2 r^{n+1} + r^{n-1} \log(r), \qquad n \text{ odd}, \tag{17}$$

which reduces to a polyharmonic spline for $c = 0$. By perturbing the polyharmonic spline by a multiple of an even power of r, we find that the result is often considerably more accurate, at the expense of poorer conditioning, than if the polyharmonic spline alone were employed. An example of the large c accuracy of the odd IMQs as well as the accuracy of the perturbed
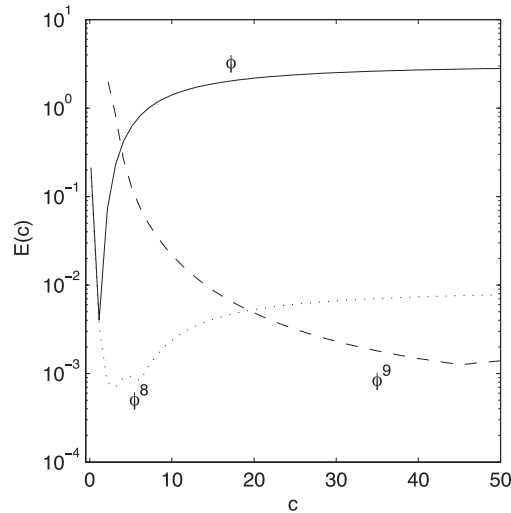

Figure 6. 1d derivative approximation of $f(x) = \exp(x^3) + \cos(2x)$ with $N = 30$ equally spaced collocation points on $[-1, 1]$. First derivative maximum error vs. shape parameter with ϕ^0 (solid), ϕ^8 (dotted), ϕ^9 (dashed).
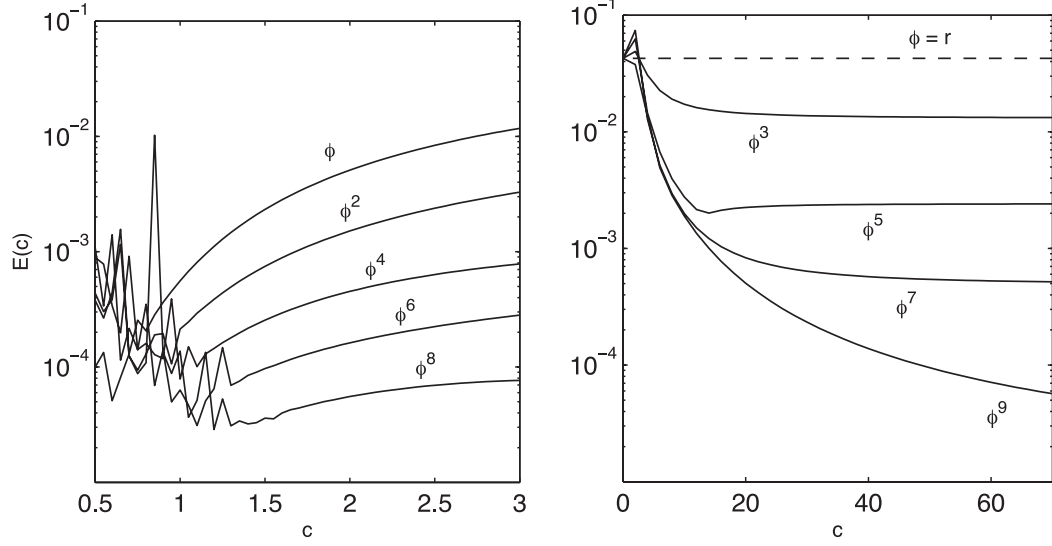
Figure 7. Interpolation maximum error vs. shape parameter with ϕ^n, n even (left) and odd (right). The function $f(x) = \exp(x^3) + \cos(2x)$ at $N = 20$ equally spaced interpolation points on $[-1, 1]$ was interpolated to a finer evenly spaced grid with $N = 100$.

polyharmonic spline (17) is illustrated for interpolation in Figure 5b. The large c accuracy of the odd IMQs is further illustrated for derivative approximation in Figure 6 and for scattered partial derivative approximation in Figure 3b.

For interpolating or derivative approximation of many functions, the IMQ approximations produce higher quality approximations over a wider range of shape parameters when compared to ϕ^0. The parent RBFs, ϕ^0, typically produce their smallest errors over a very small range of shape parameters which borders on a region of numerical instability where the condition number of the interpolation matrix exceeds the floating point limit. Since a theory which predicts the optimal shape parameter in advance does not exist, in practice a shape parameter is used which produces an interpolation matrix with condition numbers safely away from the region of instability and which does not produce the "optimal" results that are obtainable in floating point arithmetic. Often less tweaking of the shape parameter in required to achieve adequate results when using the IMQs than the MQ. Illustrating the greater accuracy of the IMQ when compared to the MQ over a wide range of the shape parameter is the example in Figure 6. The figure displays the maximum error as a function of the shape parameter from differentiating a smooth function in 1d with ϕ^0, ϕ^8, and ϕ^9 from the IMQ family. Results from interpolating a smooth function with a wide range of shape parameters are given in Figure 7.

However, at the expense of the potentially greater accuracy of the IMQs, we should expect poorer conditioning as is predicted by the uncertainty principle.

3.2. Conditioning

For a fixed value of the shape parameter, both even and odd IMQs have interpolation matrices with condition numbers that are an increasing function of the number of centers (decreasing separation distance (6)). A comparison of condition numbers with fixed shape and variable N is made among the evenly integrated MQs in Figure 8b and among oddly integrated IMQs in Figure 9b.

Even IMQs are associated with interpolation matrices that have condition numbers that are decreasing functions of the shape parameter for a fixed set of centers. The condition numbers become unbounded as $c \to 0$. For n even, numerical evidence indicates that the condition number of the interpolation matrix for all c is bounded below by the condition number of the interpolation
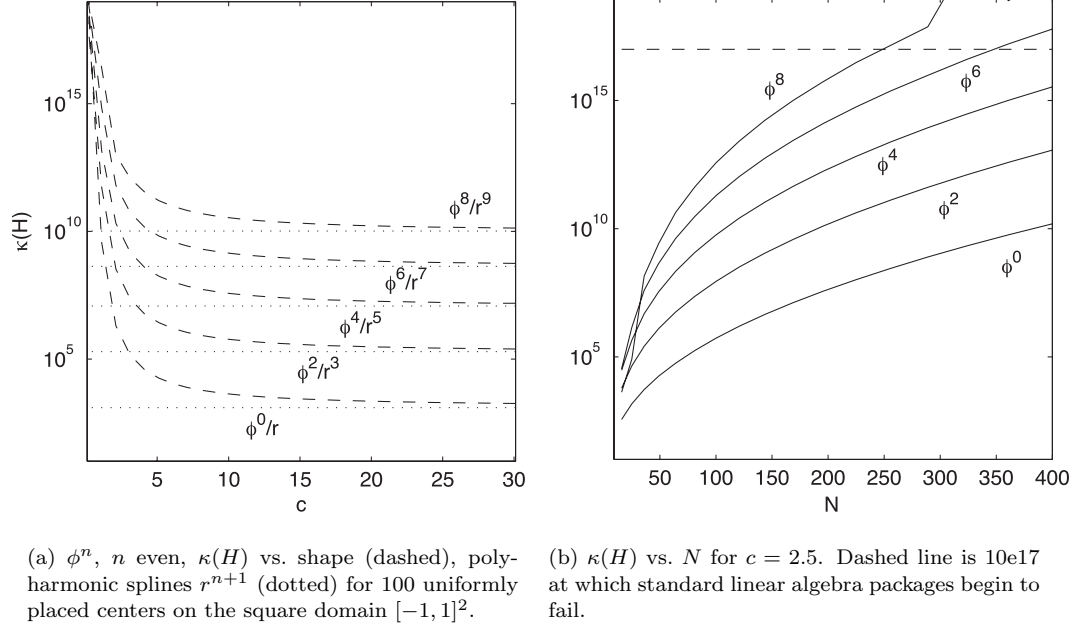
(a) ϕ^n, n even, $\kappa(H)$ vs. shape (dashed), poly-harmonic splines r^{n+1} (dotted) for 100 uniformly placed centers on the square domain $[-1, 1]^2$.

(b) $\kappa(H)$ vs. N for $c = 2.5$. Dashed line is 10e17 at which standard linear algebra packages begin to fail.

Figure 8.

(a) ϕ^n, n odd, $\kappa(H)$ vs. shape for 100 uniformly placed centers on the square domain $[-1, 1]^2$. Dotted line is the condition number of linear polyharmonic splines $\phi(r)$.

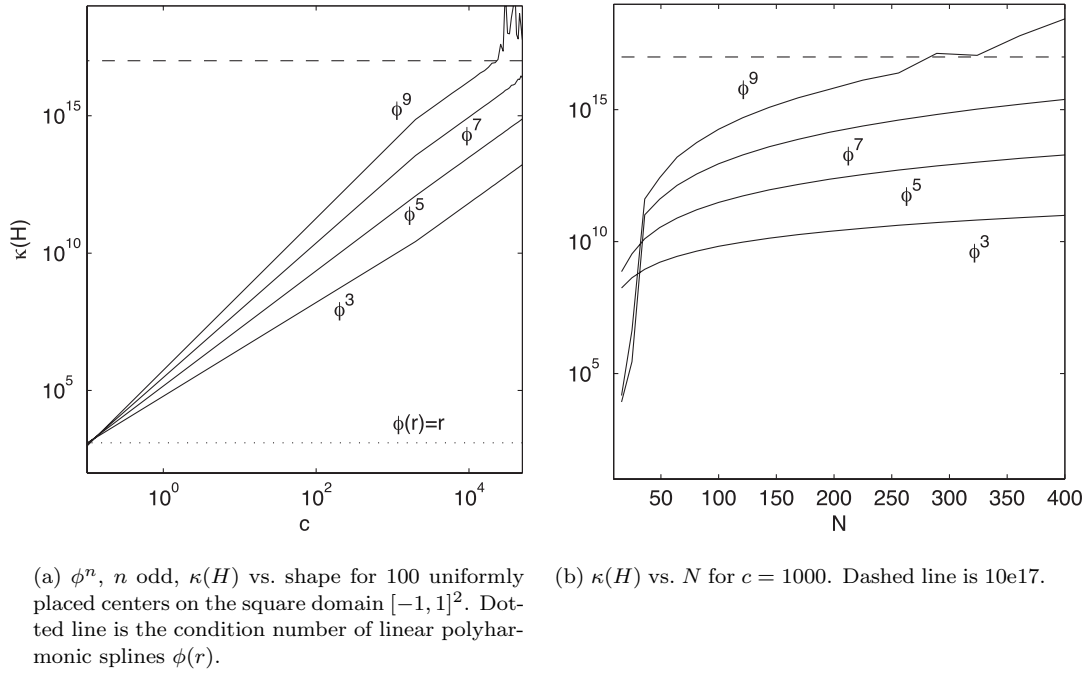(b) $\kappa(H)$ vs. N for $c = 1000$. Dashed line is 10e17.

Figure 9.

matrix of the polyharmonic spline, $\phi(r) = r^{n+1}$, that is associated with the large c approximation of the even IMQs. Thus, if the condition number of the associated polyharmonic spline exceeds the floating point limit for a particular set of centers, the IRBF will not be applicable with any value of c. Bounds for interpolation matrix condition numbers of the polyharmonic splines as well as other RBFs are discussed in [4,21–25]. The interpolation matrix condition numbers versus the shape parameter for several evenly integrated IMQs are compared Figure 8a. For reference, the condition numbers of the interpolation matrices of the associated polyharmonic splines are also shown.

Odd IMQs are associated with interpolation matrices that have condition numbers that are increasing functions of the shape parameter for a fixed number of centers. The condition numbers become unbounded as $c \to \infty$. For c sufficiently greater than zero, numerical evidence indicates that the condition numbers of the odd IMQs are bounded below by the condition number of the linear polyharmonic splines, $\phi(r) = r$. The condition number for odd IMQ interpolation matrices is compared with that of linear polyharmonic splines in Figure 9a.

4. SOLVABILITY

The theoretical results on the solvability of system (4) are based on the concept of a conditionally positive definite function. A function $\phi(r)$ is conditionally positive definite of order m in $\mathbb{R}^d$ for $d \geq 1$ if and only if

$$(-1)^\ell \frac{d^\ell}{dr^\ell} \phi\left(\sqrt{r}\right) \geq 0, \qquad \text{for } r > 0 \quad \text{and} \quad \ell \geq m.$$

If in addition, $\frac{d^m}{dr^m}\phi(\sqrt{r}) \neq$ constant, then $\phi(r)$ is conditionally strictly positive definite of order m and system (4) is uniquely solvable.

The result with $m = 0$, which establishes the solvability of system (4) for the IQ and the GA, was shown by Schoenberg in [26]. Micchelli [5] extended this result to establish the invertibility of H for RBFs that are conditionally strictly positive definite of order one, such as the MQ. This is easily verified for the MQ since $\phi(\sqrt{r}) = \sqrt{1 + c^2 r}$ and

$$(-1)^\ell \frac{d^\ell}{dr^\ell} \phi\left(\sqrt{r}\right) = \frac{\Gamma(\ell - 1/2)c^{2\ell}}{2\sqrt{\pi}\left(1 + c^2 r\right)^{\ell - 1/2}} > 0, \qquad \text{for } r > 0 \quad \text{and} \quad \ell \geq 1. \tag{18}$$

Micchelli further extended the theory in [5] to include RBFs that are conditionally strictly positive definite of order $m \geq 2$. This was accomplished by placing some mild restrictions on the center locations and by adding polynomial terms to the basic RBF interpolation problem. With the addition of polynomial terms we have the augmented RBF interpolant

$$s(x) = \sum_{i=0}^{N} \lambda_i \phi\left(\|x - x_i\|\right) + \sum_{j=1}^{M} \gamma_j p_j(x), \qquad x \in \mathbb{R}^d. \tag{19}$$

The additional constraints are

$$\sum_{i=0}^{N} \lambda_i p_j(x_j) = 0, \qquad j = 1, 2, \ldots, M, \tag{20}$$

where $\{p_j(x)\}_{j=1}^{M}$ is a basis for the M-dimensional space, Π_m^d, of algebraic d-variate polynomials that are of degree less than or equal to m. Examples of strictly positive definite RBFs of order m are the polyharmonic splines $\phi(r) = (-1)^m r^k$ where $2m - 2 < k < 2m$ and $\phi(r) = (-1)^m r^{2m-2} \log r$.

We can verify that the IMQs are not conditionally strictly positive definite of order m for any $m < \lfloor(n+2)/2\rfloor$. It is difficult to show rigorously that the IMQs are conditionally strictly positive definite of order $m \geq \lfloor(n+2)/2\rfloor$ as we are unable to obtain a simple expression for the derivatives of $\phi^n(\sqrt{r})$ as is possible for the MQ in equation (18) due to the more complicated structure of the IRBFs. Graphically, it can be verified that the IMQs are conditionally strictly positive definite of order $m = \lfloor(n + 2)/2\rfloor$. This is the same order m as the associated polyharmonic spline of the even IMQs and the polyharmonic spline portion of the large c approximation (17) of the odd IMQs.

In our numerical experiments, a singular H was never encountered when the IMQ methods were not augmented with polynomials. When polynomial terms were added, they did not significantly

improve, and in many cases lessened, the accuracy of the approximants unless the function being approximated was a polynomial.

5. NUMERICAL RESULTS

As a numerical example, we take test problem 1 from [27], the two-dimensional Poisson problem

$$u(x) = g(x), \qquad \text{on } \partial\Omega,$$

$$\Delta u(x) = f(x), \qquad \text{in } \Omega,$$

$$(21)$$

on the unit circle Ω with the exact solution

$$u_1 = \frac{65}{(65 + (x_1 - 0.2)^2 + (x_2 + 0.1)^2)}.$$

Kansa's asymmetric collocation method [1] on $N = 54$ centers distributed as in Figure 4 is used to solve the problem. The linear system which arises when using the asymmetric method to solve problem (21) is of the form

$$A\lambda = F,$$

where

$$A = \begin{bmatrix} \phi \\ \hline \Delta\phi \end{bmatrix}, \qquad F = \begin{bmatrix} g \\ \hline f \end{bmatrix}.$$

The set of collocation points Ξ is split into a set $\mathcal{I}$ of interior points, and $\mathcal{B}$ of boundary points. The two blocks of the matrix A are generated as

$$\phi_{ij} = \phi\left(\|x_i - x_j\|_2\right), \qquad x_i \in \mathcal{B}, \quad x_j \in \Xi,$$

$$\Delta\phi_{ij} = \Delta\phi\left(\|x_i - x_j\|_2\right), \qquad x_i \in \mathcal{I}, \quad x_j \in \Xi.$$

After the coefficients λ are found, the approximate solution is computed via (2). The nonsingularity results for the interpolation matrices do not carry over to the asymmetric collocation method. The addition of polynomial terms no longer guarantees the invertibility of the coefficient matrix. For certain configurations, it was demonstrated in [28] that the collocation matrix may

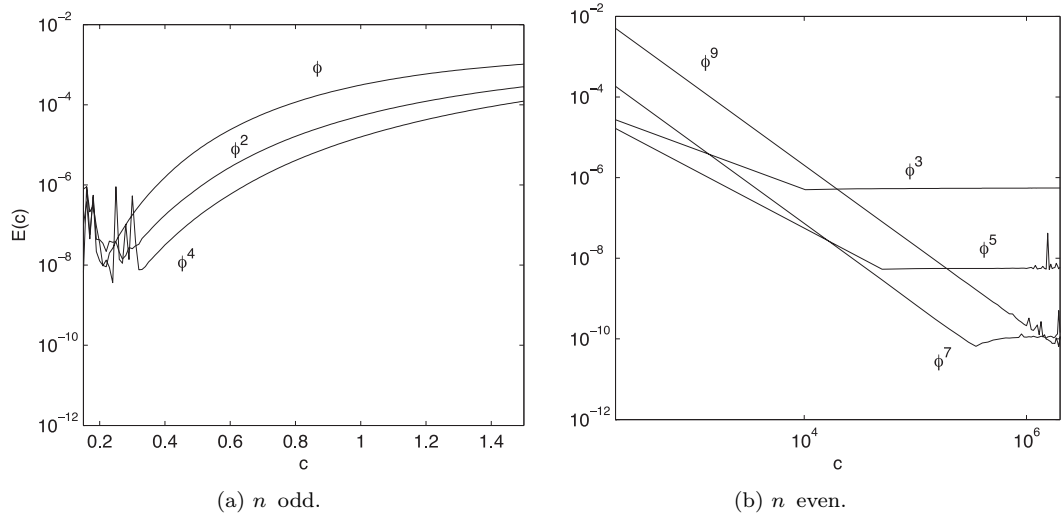(a) n odd.   (b) n even.

Figure 10. 2d Poisson problem on scattered centers. Max errors vs. shape parameter from solving $\Delta u = f$ with center distribution pictured in Figure 8 on the unit circle using ϕ^n from the IMQ family.

be singular. Despite the fact that Kansa's method cannot be shown to be well posed, it rarely produces singular matrices in practice and has been widely successful in applications [29].

The maximum errors resulting from the asymmetric collocation method applied to test problem 1 with solution u_1 using IMQs over a wide range of shape parameters are shown in Figure 10. The results using ϕ^n, n even, in the left image shows that the IMQs produce a smaller error over a wide range of the shape parameter than the standard RBF produces. As c gets small and the region of ill-conditioning is approached all the even members of the family approach approximately the same minimum error. The IMQs realize their smallest error for larger c than the MQ. In this particular example, the oddly integrated results shown in the loglog plot in Figure 10b are particularly impressive. IMQ ϕ^7 produces the smallest error of 6.5e−11 with $c = 3.5e+5$ which is several decimal places more accurate than the best evenly integrated result using ϕ^4 with $c = 0.32$ which produces an error of 7.7e−9. Ill-conditioning prevented obtaining better results with ϕ^6 or ϕ^8 than we obtained with ϕ^4.

In [27], five additional functions were used as exact solutions to (21) which required very different optimal values of the shape parameter due to the varying smoothness of the solutions. The IRBF results for test problems two to six were not quite as impressive, as the IMQ minimum errors were not substantially better than the standard MQ results as in problem 1. However, the IMQs typically achieved a smaller error over a larger range of the shape parameter than did the MQ. This is perhaps the major advantage of the IRBFs as RBF methods are typically not employed in applications using the optimal shape parameters, but using some value of the parameter safely away from the region of ill-conditioning. Obviously, finding the optimal shape parameter in applications by brute force, using standard algorithms or the Contour-Padé algorithm, is impossible as an exact solution is seldom known.

6. CONCLUSIONS

Radial basis function approximation methods that use integrated families of RBFs have been described. The MQ RBF was used as the parent of the family, but other RBFs such as the IQ or GA could be used as well. Members of the IRBF family are found by integrating the parent RBF n times with respect to r. The properties of the resulting methods depend on whether n is even or odd. We did not consider the case $n > 9$, but we do not discount the utility of doing so.

For n even, the methods behave as those based on the parent RBF. That is, they are generally most accurate and most poorly conditioned for small values of the shape parameter c. For n odd, the methods are most accurate and most poorly conditioned for large c. A summary of properties is listed in Table 2.

Numerical results indicate that when compared to the MQ method, the IMQ approximation methods may produce significantly more accurate results over a wide range of shape parameters. The IMQ methods are also more poorly conditioned than the MQ method. While it is largely uncertain which choice of RBF will produce the most accurate result for a particular

Table 2. Summary of IRBF properties.

	n Even	n Odd
$\kappa(H)$ as $c \to 0$, N fixed	∞	$\kappa(H)$ for $\phi(r) = r$
$\kappa(H)$ as $c \to \infty$, N fixed	$\kappa(H)$ for $\phi(r) = r^{n+1}$	∞
1d interpolant as $c \to 0$	$\phi^0 \equiv$ Lagrange interpolant	$\phi(r) = r$
Interpolant as $c \to 0$, $d > 1$	Depends on ϕ^n	$\phi(r) = r$
Large c interpolant	$\phi(r) = r^{n+1}$	$\phi(r) = c^2 r^{n+1} + r^{n-1} \log r$

approximation problem, RBFs that have been integrated several times appear to be superior to standard nonintegrated RBFs when the function being approximated is sufficiently smooth. The IRBFs may be most valuable for approximating smooth functions in higher dimensions where the IRBFs could possibly use significantly fewer centers than their parents to achieve the same approximation accuracy.

REFERENCES

1. E. Kansa, Multiquadrics—A scattered data approximation scheme with applications to computational fluid dynamics I: Solutions to parabolic, hyperbolic, and elliptic partial differential equations, *Computers Math. Applic.* **19** (8/9), 147–161, (1990).
2. E. Kansa, Multiquadrics—A scattered data approximation scheme with applications to computational fluid dynamics I: Surface approximations and partial derivative estimates, *Computers Math. Applic.* **19** (8/9), 127–145, (1990).
3. H. Wendland, Piecewise polynomial, positive definite and compactly supported radial functions of minimal degree, *Advances in Computational Mathematics* **4**, 389–396, (1995).
4. M.D. Buhmann, *Radial Basis Functions*, Cambridge University Press, (2003).
5. C. Micchelli, Interpolation of scattered data: Distance matrices and conditionally positive definite functions, *Constructive Approximation* **2**, 11–22, (1986).
6. R. Schaback, Error estimates and condition numbers for radial basis function interpolation, *Advances in Computational Mathematics* **3**, 251–264, (1995).
7. T.A. Foley, Near optimal parameter selection for multiquadric interpolation, *Journal of Applied Science and Computation* **1**, 54–69, (1994).
8. R.L. Hardy, Theory and applications of the multiquadric-biharmonic method, *Computers Math. Applic.* **19** (8/9), 163–208, (1990).
9. S. Rippa, An algorithm for selecting a good value for the parameter c in radial basis function interpolation, *Advances in Computational Mathematics* **11**, 193–210, (1999).
10. M.-D. Nam and T.-C. Thanh, Numerical solution of differential equations using multiquadric radial basis functions networks, *Neural Networks* **14**, 185–199, (2001).
11. M.-D. Nam and T.-C. Thanh, Numerical solution of Navier-Stokes equations using multiquadric radial basis functions networks, *International Journal for Numerical Methods in Fluids* **37**, 65–86, (2001).
12. M.-D. Nam and T.-C. Thanh, Approximation of function and its derivatives using radial basis functions networks, *Applied Mathematical Modelling* **27**, 197–220, (2003).
13. W.R. Madych and S.A. Nelson, Multivariate interpolation and conditionally positive definite functions, *Approximation Theory and Its Applications* **4** (4), 77–89, (1988).
14. W.R. Madych, Miscellaneous error bounds for multiquadric and related interpolators, *Computers Math. Applic.* **24** (12), 121–138, (1992).
15. L. Ling and M.R. Trummer, Multiquadric collocation method with integral formulation for boundary layer problems, *Computers Math. Applic.* **48** (5/6), 927–941, (2004).
16. E.J. Kansa, H. Power, G.E. Fasshauer and L. Ling, A volumetric integral radial basis function method for time-dependent partial differential equation: I. Formulation, *Journal of Engineering Analysis with Boundary Elements* (to appear).
17. T. Driscoll and B. Fornberg, Interpolation in the limit of increasingly flat radial basis functions, *Computers Math. Applic.* **43** (3–5), 413–422, (2002).
18. E. Larsson and B. Fornberg, Theoretical and computational aspects of multivariate interpolation with increasing flat basis functions, *Computers Math. Applic.* **49** (1), 103–130, (2005).
19. R. Schaback, Multivariate interpolation by polynomials and radial basis functions, pp. 1–21, Preprint, (2002).
20. B. Fornberg and G. Wright, Stable computation of multiquadric interpolants for all values of the shape parameter, *Computers Math. Applic.* **48** (5/6), 853–867, (2004).
21. K. Ball, N. Sivakumar and J.D. Ward, On the sensitivity of radial basis interpolation to minimal data separation distance, *Constructive Approximation* **8**, 401–426, (1992).
22. F.J. Narcowich, N. Sivakumar and J.D. Ward, On the condition numbers associated with radial basis interpolation, *Journal of Mathematical Analysis and Applications* **186**, 457–485, (1994).
23. F.J. Narcowich and J.D. Ward, Norms of inverses and condition numbers for matrices associated with scattered data, *Journal of Mathematical Analysis and Applications* **186**, 457–485, (1994).
24. R. Schaback, Lower bounds for norms of inverses of interpolation matrices for radial basis functions, *Journal of Approximation Theory*, 1–14, (1900).
25. R. Schaback, Error estimates and condition numbers for radial basis function interpolation, *Advances in Computational Mathematics* **3**, 251–264, (1995).
26. I.J. Schoenberg, Metric spaces and completely monotone functions, *Annals of Mathematics* **39**, 811–841, (1938).
27. E. Larsson and B. Fornberg, A numerical study of some radial basis function based solution methods for elliptic PDEs, *Computers Math. Applic.* **46** (5/6), 891–902, (2003).

28. Y. Hon and R. Schaback, On nonsymmetric collocation by radial basis function, *Applied Mathematics and Computation* **119**, 177–186, (2001).
29. E. Kansa and Y.C. Hon, Circumventing the ill-conditioning problem with multiquadric radial basis functions: Applications to elliptic partial differential equations, *Computers Math. Applic.* **39** (7/8), 123–137, (2000).